Title

A new immunodeficient pigmented retinal degenerate rat strain to study transplantation of human cells without immunosuppression

Journal

Graefe's Archive for Clinical and Experimental Ophthalmology, 252(7)

ISSN

0941-2921

Authors

Seiler, Magdalene J

Aramant, Robert B

Jones, Melissa K

et al.

Publication Date

2014-07-01

DOI

10.1007/s00417-014-2638-y

Peer reviewed

Graefes Arch Clin Exp Ophthalmol (2014) 252:1079–1092
DOI 10.1007/s00417-014-2638-y

BASIC SCIENCE

A new immunodeficient pigmented retinal degenerate rat strain to study transplantation of human cells without immunosuppression

Magdalene J. Seiler · Robert B. Aramant · Melissa K. Jones · Dave L. Ferguson · Elizabeth C. Bryda · Hans S. Keirstead

Received: 6 January 2014 / Revised: 26 March 2014 / Accepted: 7 April 2014 / Published online: 13 May 2014

Abstract
Purpose The goal of this study was to develop an immunodeficient rat model of retinal degeneration (RD nude rats) that will not reject transplanted human cells.
Methods SD-Tg(S334ter)3Lav females homozygous for a mutated mouse rhodopsin transgene were mated with NTac:NIH-*Whn* (NIH nude) males homozygous for the *Foxn1*^{rnu} allele. Through selective breeding, a new stock, SD-Foxn1 Tg(S334ter)3Lav (RD nude) was generated such that all animals were homozygous for the *Foxn1*^{rnu} allele and either homo- or hemizygous for the S334ter transgene. PCR-based assays for both the *Foxn1*^{rnu} mutation and the S334ter transgene were developed for accurate genotyping. Immunodeficiency was tested by transplanting sheets of hESC-derived neural progenitor cells to the subretinal space of RD nude rats, and, as a control, NIH nude rats. Rats were killed between 8 and 184 days after surgery, and eye sections were analyzed for human, neuronal, and glial markers.
Results After transplantation to RD nude and to NIH nude rats, hESC-derived neural progenitor cells differentiated to neuronal and glial cells, and migrated extensively from the transplant sheets throughout the host retina. Migration was more extensive in RD nude than in NIH nude rats. Already 8 days after transplantation, donor neuronal processes were found in the host inner plexiform layer. In addition, host glial cells extended processes into the transplants. The host retina showed the same photoreceptor degeneration pattern as in the immunocompetent SD-Tg(S334ter)3Lav rats. Recipients survived well after surgery.
Conclusions This new rat model is useful for testing the effect of human cell transplantation on the restoration of vision without interference of immunosuppression.

Keywords Photoreceptor degeneration · Immunodeficiency · Retinal transplantation · Xenografts · Human embryonic stem cells · Human neural progenitor cells · Rat strain

Abbreviations

hESC	Human embryonic stem cells
RD	Retinal degeneration
GC	Ganglion cell layer
IP	Inner plexiform layer
IN	Inner nuclear layer
ON	Outer nuclear layer
RPE	Retinal pigment epithelium
H	Host
T	Transplant
CRALBP	Cellular retinaldehyde binding protein
GFAP	Glial fibrillary acidic protein
NF	Neurofilament
MAP	Microtubule-associated protein

M. J. Seiler · R. B. Aramant · M. K. Jones · D. L. Ferguson · H. S. Keirstead
Anatomy & Neurobiology/Reeve-Irvine Research Center, University of California, Irvine, CA, USA

M. K. Jones
Department of Biomedical Sciences/Regenerative Medicine Institute, Cedars-Sinai Medical Center, Los Angeles, CA, USA

M. K. Jones
Department of Biological Sciences, California State University Long Beach, Long Beach, CA, USA

E. C. Bryda
Rat Resource and Research Center, University of Missouri, Columbia, MO, USA

H. S. Keirstead (✉)
Reeve-Irvine Research Center, Sue and Bill Gross Stem Cell Research Center, School of Medicine, University of California at Irvine, Irvine, CA, USA
e-mail: hans@californiastemcell.com

NRL	Neural retina-specific leucine zipper protein
Otx2	Orthodenticle homolog 2 homeobox protein
PKC	Protein kinase C
RA	Retinoic acid
HA	Hyaluronic acid
IST	Insulin/Selenite/Transferrin
T3	Triiodothyronine

degeneration rate as the original SD-Tg(S334ter)3Lav rats. Immunodeficiency was tested by analyzing transplants of ESC-derived neural progenitor cell sheets to the subretinal space up to 6 months (176–184 days) after surgery. Our data show that this new strain is useful for xenografting human cells without immunosuppression.

Introduction

Diseases of photoreceptors and retinal pigment epithelium (RPE), such as retinitis pigmentosa and age-related macular degeneration, affect millions of people and lead to irreversible vision loss [1–5]. Current treatment approaches, such as nutritional supplements [6], growth factors [7–9], transplantation of RPE [10, 11], or retinal progenitors [12] target early disease stages with the aim to delay retinal degeneration and do not aim to replace lost photoreceptors. Replacing photoreceptors with transplants of dissociated photoreceptor precursors has been demonstrated, but the cells can only develop full photoreceptor morphology when a photoreceptor layer is still present [13–15] and do not survive long term because they can elicit immune responses [16]. In contrast, transplantation of fetal-derived retinal sheets (with and without its RPE) has shown long-term photoreceptor replacement and visual restoration in animal models [17–19] and visual improvements in phase 2 clinical trials [20]. However, since the supply of fetal tissue is limited and its use controversial, an alternative source of donor tissue is needed. Several groups are working on differentiating human (embryonic or induced) pluripotent stem cells into retinal progenitors and photoreceptors [21–28].

To demonstrate efficacy, human stem cell-derived retinal cells can be transplanted as xenografts to animal models of retinal degeneration. However, xenografts require immunosuppression or an immunodeficient host. Chemical immunosuppression may negatively influence transplant differentiation and survival and is very labor-intensive.

Therefore, we sought to create an immunodeficient rat model of retinal degeneration, derived from a cross between transgenic retinal degenerate rats and athymic nude rats. Transgenic rats expressing mutant rhodopsins with varying rates of photoreceptor degeneration had been created in the 1990s [29–31]. The SD-Tg(S334ter)3Lav transgenic stock was selected because it shows a relatively fast degeneration rate [31] both in homozygotes and hemizygotes, and has been used in previous experiments. Athymic nude rats carry a mutation of the *Foxn1* gene and do not have T-cells [32, 33]. These rats have been used in many transplantation studies [34–37]. Crossing both strains resulted in immunodeficient rats that showed the same retinal

Materials and methods

Experimental animals

For all experimental procedures, animals were treated in accordance with the NIH guidelines for the care and use of laboratory animals and the ARVO Statement for the Use of Animals in Ophthalmic and Vision Research, and under a protocol approved by the Institutional Animal Care and Use Committee of UC Irvine.

Founder breeders of S334ter line 3 transgenic rats [Tg(S334ter)3Lav] were received as a gift from Dr. Matthew LaVail (UCSF) in 1999. The rats were originally produced by Chrysalis DNX Transgenic Sciences, now Xenogen Biosciences (Princeton, NJ, USA). The transgene carried by these rats contains a mutant mouse rhodopsin (*Rho*) gene with a terminal stop codon affecting residue 334. This results in a protein that lacks the terminal 15 amino acids and thus all the phosphorylation sites [29–31].

The breeding scheme is shown in Fig. 1. SD-Tg(S334ter)3Lav animals were bred to NTac:NIH-*Whn* (NIH nude) rats from Taconic (Rensselaer, NY, USA) in a breeding contract with Taconic. The resulting stock, SD-Foxn1 Tg(S334ter)3Lav, was donated to the Rat Resource and Research Center (RRRC) at the University of Missouri (www.rrrc.us) where it was re-derived for distribution (RRRC #539). The $Foxn1^{rnu}$ mutation carried by NIH nude rats results in T-cell deficiency and immunodeficiency. Since homozygous nude ($Foxn1^{rnu}/Foxn1^{rnu}$) females are poor breeders [38] , the strain was maintained by intra-strain mating between heterozygous $+/Foxn1^{rnu}$, S334ter transgene (Tg)-positive females to either homozygous ($Foxn1^{rnu}/Foxn1^{rnu}$) or heterozygous ($+/Foxn1^{rnu}$) S334ter Tg-positive males (see Fig. 1, breeding scheme). This provided rats suitable for study that were both homozygous nude and Tg positive (immunodeficient and retinal degenerate). The new strain, SD-Foxn1Tg(S334ter)3LavRrrc (RRRC#539), as well as the original strain, SD-Tg(S334ter)3Lav (RRRC#643), are available through the Rat Resource and Research Center at the University of Missouri (www.rrrc.us) as cryopreserved embryos and sperm. Rats maintained at Taconic and at the RRRC were housed in microisolators.

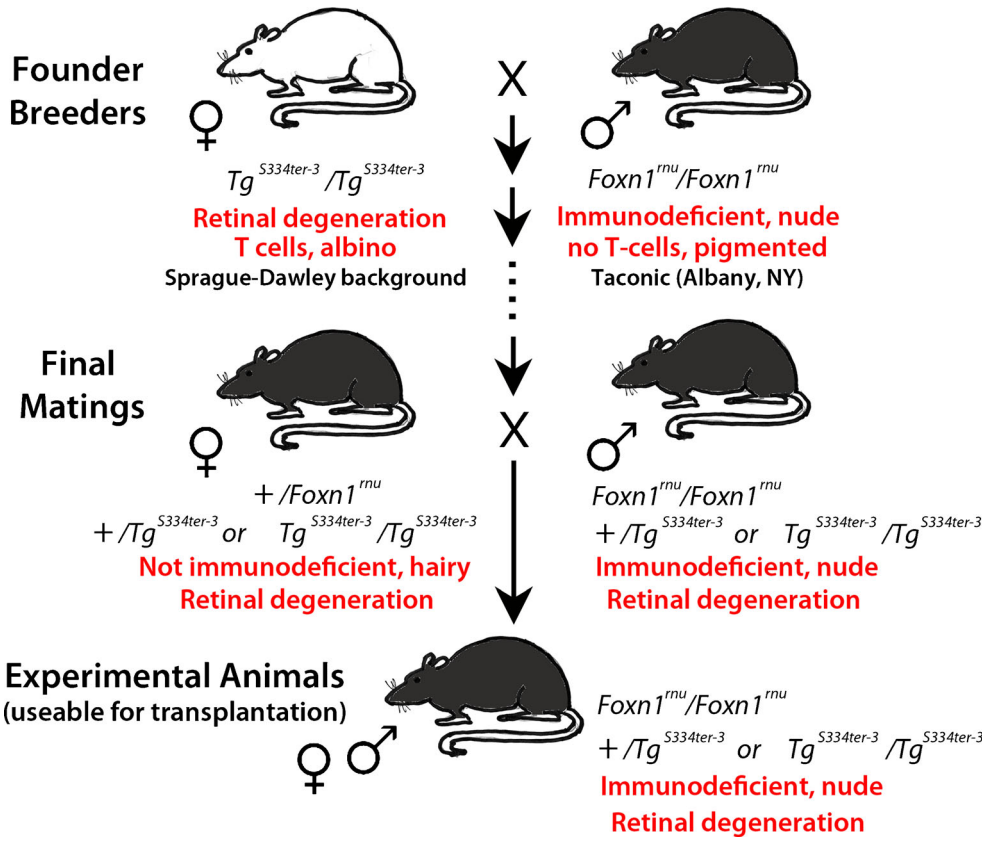

Fig. 1 Schematic diagram of breeding strategy. Founder breeders were albino SD-Tg(S334ter)3Lav homozygous transgene-positive ($Tg^{S334ter}$) females and pigmented homozygous nude (*Foxn1*^{rnu}/*Foxn1*^{rnu}) males. After selective breeding, a new rat stock was generated consisting of pigmented animals that carried the S334ter-3 transgene, and were either homo- or heterozygous for the *Foxn1*^{rnu} allele. Heterozygous +/*Foxn1*^{rnu}, transgene-positive females were bred with homozygous *Foxn1*^{rnu}/*Foxn1*^{rnu}, transgene-positive males to provide homozygous nude Tg S334ter-positive rats suitable for xenografting (RD nude rats)

Genotyping

Assays for both the *Foxn1* nude mutation and the S334ter transgene were developed for accurate genotyping of animals. DNA was extracted from tail biopsies using the DNeasy Blood and Tissue kit (Qiagen, Valencia, CA, USA) following the manufacturer's protocol.

For determining the presence of the S334ter-transgene, 20-μl PCR reactions were set up with 10 μl of Ext-n-amp Solution (Sigma, St. Louis, MO, USA), 0.3 μl of each 25 μM primer and 40 ng of genomic DNA. Primer sequences were R539A: 5′-TGG GAG ATG ACG ACG CCT AA-3′ and R539B: 5′-TGA GGG AGG GGT ACA GAT CC-3′. Thermal cycling conditions were: 1 cycle of 94 °C for 5 min; 35 cycles of 94 °C for 30 s, 66 °C for 30 s, and 72 °C for 1 min; 1 cycle of 72 °C for 10 min. The expected amplicon is 350 bp. All samples were analyzed by capillary electrophoresis on a QIAxcel (Qiagen) with the QIAxcel DNA Screening Kit, QX Alignment Marker 15 bp/1 kb and QX DNA Size Marker 50–800 bp. Conditions were as follows: method, AM320 injection: 10s at 5KV, separation: 320 s at 6KV (see Fig. 2a).

For detecting the single base pair change (C to T) at nucleotide 1429 of the *Foxn1* gene, a TaqMan assay was developed. Primers R363F 5′-GCAGACCTACCCACACCT TTCTC-3′ and R363R 5′-CTGGGCCTGCAGATCAAGAT-3′ and probes R363A (FAM-labeled) 5′-CAT TGT TTT CAt AGC CAG A-3′ and R363B (VIC-labeled) 5′-CAT TGT TTT CAc AGC CAG-3′ were used. The *lowercase letter* indicates the base pair found in the wild-type allele (detected by probe R363B) or the mutant allele (detected by probe R363A). The probes were ordered from Applied Biosystems (St. Louis, MO, USA). Twenty-microliter PCR reactions consisting of 20 ng genomic DNA, 2X TaqMan Universal Master Mix (Applied Biosystems), 0.9 μM of each primer, and 0.2 μM of each probe were performed in an ABI Prism 7000 Sequence Detection system (Applied Biosystems) with the following thermal cycling conditions: 50 °C for 2 min; 95 °C for 10 min; 40 cycles of 95 °C for 15 s, 60 °C for 1 min. Allelic discrimination analysis was performed with the ABI 7000 SDS software (see Fig. 2b).

Differentiation of hESC-derived neural progenitor cells

Human embryonic stem cells (hESCs) of the H7 line were differentiated into neural progenitor cell sheets (in laminin, collagen matrix) (after [39]). Cells were expanded on Matrigel (BD Biosciences, San Jose, CA, USA) using conditioned media by a mitotically inactivated mouse fibroblast feeder layer, containing 10 ng/ml FGF. The cells were passaged every 5–7 days using 1 mg/ml collagenase IV (Invitrogen, Carlsbad, CA, USA) with a splitting ratio of 1:4 to 1:6.

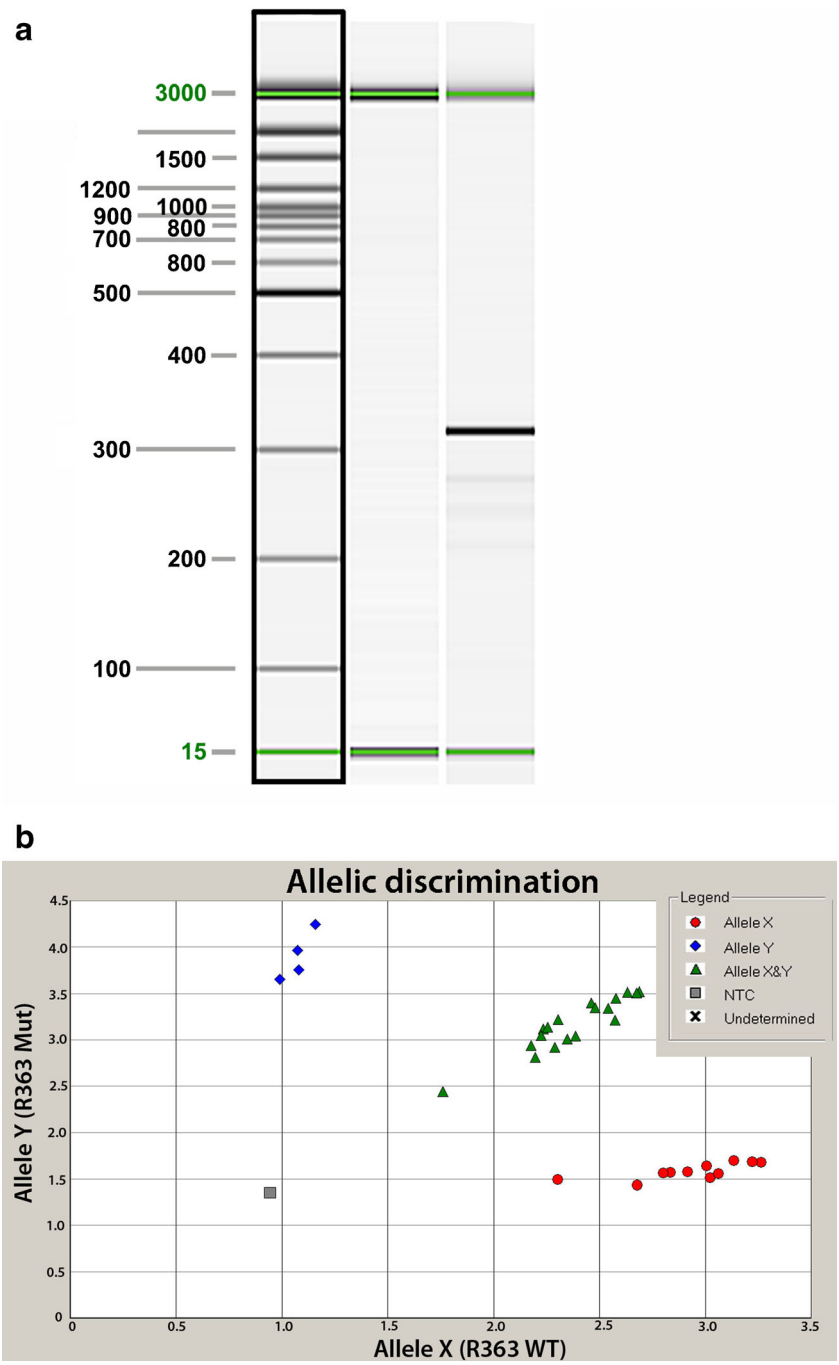

Fig. 2 Genotyping assays. **a** S334ter transgene genotyping assay. *Lane 1* 15 bp–3 kb size marker. *Lane 2* transgene-negative sample. *Lane 3* transgene-positive sample. Sizes in base pairs (bp) are indicated to the left of the image. An amplicon of 350 bp indicates the presence of the transgene. The 15- and 3,000-bp alignment markers are present in all lanes. **b** Allelic discrimination assay plot for detection of the *Foxn1*^{rnu} mutation. The fluorescence levels of VIC (wild type, allele X) and FAM (mutant, allele Y) are plotted on the *x* and *y* axes, respectively. The genotypes of each sample are represented by *blue diamonds* (homozygous *Foxn1*^{rnu}), *red circles* (homozygous for the wild-type *Foxn1* allele) or *green triangles* (heterozygous +/*Foxn1*^{rnu}). The no template negative control is represented by the *gray box*

After reaching 75–100 % confluence, hESC cells were induced to differentiate in non-adherent flasks by exposing the cells to "induction media" (serum-free) consisting of DMEM/F12 high-glucose, B27 supplement, Insulin-Selenite-Transferrin (IST), triiodothyronine (T3), Taurine 2.5 g/l; hyaluronic acid (HA) 250 mg/l; Dickkopf-1 (Dkk) 25 ng/ml, LeftyA (TGF-beta ligand and antagonist of Nodal signaling) 50 ng/ml, FGF 5 ng/ml (Invitrogen, Carlsbad, CA, USA). Retinoic acid (RA, 10 μM) was added from day 10 to 13, diluted from a 20 mM stock solution in dimethyl sulfoxide (DMSO; Sigma, St. Louis, MO, USA). Cells were fed every 2nd day. Formation of cell aggregates (embryoid bodies) was observed after day 7. On day 21, cells were dissociated by collagenase and replated on adherent dishes coated with Laminin and collagen type 1, in "maintenance media" (DMEM/F12 high-glucose, B27, IST, T3, Taurine 2.5 g/l; hyaluronic acid 250 mg/l, FGF 5 ng/ml) and cultured until day 36–44. Cells formed multilayered sheets of varying thickness.

Transplantation of hESC-derived neural progenitor cells

Neural progenitor sheets were placed into cold Hibernate E medium, and stored on ice for up to 6–8 h. Sheets were detached from the dish using a specially made spatula, and cut into rectangular pieces of 1.0–1.3 mm^2 as measured with a micro-measurement tool. Before transplantation, the tissue was picked up into the flat plastic nozzle of a custom-made implantation instrument (U.S. Patents # 5,941,250; # 5,941,250; and # 6,156,042; described in detail in [40]). The tissue was cut exactly to the space in the nozzle tip, and was inserted flat (not rolled up) into the nozzle tip. The instrument has a fixed plunger/mandrel and a moveable flat nozzle. The volume in the nozzle tip can be pre-determined, and the nozzle can be locked in place with the loaded tissue.

Sheets were transplanted to the subretinal space of 12 RD nude rats (39–45 days old), and, as a control, eight homozygous NIH nude (*Foxn1*^{rnu}/*Foxn1*^{rnu}) rats (43–51 days old). Rats were anesthetized by i.p. injection of ketamine/xylazine (37.5 and 5 mg/kg), and pupils dilated by Atropine eye drops (Akorn Pharmaceuticals, Lake Forest, IL, USA). The right eye served as non-surgery control and was covered by artificial tears ointment (Fougera Pharmaceuticals, Melville, NY, USA). The superior area of the left eye between two varicose veins was exposed. A small incision (0.5–1 mm) was cut behind the pars plana. The loaded implantation instrument was inserted into the subretinal space and advanced further, nasal to the optic disc. After reaching the target area, hESC-derived sheets were placed into the subretinal space and the instrument withdrawn. The incision site was closed with 10–0 sutures, and the cornea covered with artificial tears ointment. Rats were recovered from anesthesia in a Thermocare incubator. Rats were housed in sterile microisolator cages.

Histology and immunohistochemistry

ESC-derived neuronal progenitor sheets not used for transplantation were fixed with 4 % paraformaldehyde, infiltrated with 30 % sucrose, and frozen in OCT (optimal cutting compound) in isopentane on dry ice for 10-μm cryostat sections.

Rats were killed between 8 and 184 days after surgery (age 51–227 days = 1.7 to 7.4 months), and perfusion-fixed. Dissected eye cups were post-fixed with cold 4 % paraformaldehyde in 0.1 M Na-phosphate buffer for several hours. After washing with 0.1 M Na-phosphate buffer and further dissection, eye cups were infiltrated with 30 % sucrose, and frozen in OCT. Dissected eye cups were photographed and transplant sizes (thickened retinal area) were measured before embedding. Cryostat sections [cross sections along the dorso-ventral (superior-inferior) axis] were incubated in HistoVT One (Nacalai Inc., San Diego, CA, USA; 1:10 dil., 20–30 min. at 70 °C) for antigen retrieval, washed with PBS (phosphate buffered saline: 0.1 M NaCl, 0.05 M Na-phosphate buffer, pH 7.2), blocked for at least 30 min in 20 % goat serum, and incubated with various antibodies overnight at 4 °C (Table 1). After 3× washing with PBS, fluorescent secondary antibodies (1:200, Invitrogen [Molecular Probes]) were used for at least 30 min at room temperature. After further washing with PBS, sections were coverslipped using DAPI (4′6′-diamidino-2-phenylinode hydrochloride) containing Vectashield mounting medium (Vector Labs) to label nuclei blue fluorescent. Sections were imaged using a Nikon FXA fluorescent microscope or a LSM710 confocal microscope with settings for DAPI, FITC, and TRITC.

Results

Breeding and genotyping of new rat strain

It took about 10 months (from April 2009 to February 2010) and several crosses and back-crosses to consistently produce rats that were both homozygous for the *Foxn1*^{rnu} allele and carried the S334ter-3 transgene (Fig. 1). Animals were genotyped for the S334ter transgene and the *Foxn1*nude mutation using PCR-based assays (Fig. 2a, b) but additionally, the homozygous nude phenotype could be determined by visual inspection of the rats. Homozygous *Foxn1*^{rnu} rats are hairless, but heterozygous *Foxn1*^{rnu} rats have hair. Because homozygous nude females are poor breeders, heterozygous +/*Foxn1*^{rnu}, transgene-positive females were bred with homozygous *Foxn1*^{rnu}/*Foxn1*^{rnu}, transgene-positive males to provide homozygous nude Tg S334ter-positive rats (RD nude) suitable for study. Rats were bred further by Taconic until April 2011 before being donated to the RRRC where they were re-derived for distribution.

Retinal degeneration in RD nude rats

Once the new rat stock (RD nude) was established, 12 RD nude rats were shipped and used for transplantation in one eye. Non-surgery eyes of these RD nude rats were analyzed by immunohistochemistry for various retinal markers at the ages of 1.7 to 7.4 months (51 to 221 days). At the age of 1.7 months, rods had almost completely disappeared (Fig. 3a), although a few rhodopsin immunoreactive cells with abnormal morphology were still remaining at the age of 7.4 months (Fig. 3j). A progressive loss of cones was observed by immunohistochemistry for recoverin (Fig. 3a, d, g, j), RG opsin (Fig. 3b, e, h, k), and arrestin (Fig. 3c, f, i, l). Extensive retinal remodeling was present at the age of 7.4 months (Fig. 3j, k, l). This degeneration is similar to the original standard Tg strain, immunocompetent hemizygous pigmented SD-Tg(S334ter)3Lav rats [31].

Table 1 Antibodies used in the study

Antibody specificity	Species	Specific for	Dilution	Source
Primary antibodies				
Arrestin (S-antigen, clone A9C6)	Mouse	Rod and cone photoreceptors	1:1000	Gift of Dr. Donoso, Philadelphia Retina Endowment Fund, PA [57]
beta-III-tubulin	Rabbit	Processes of early neurons	1:250	Epitomics, Burlingame, CA
Chx10 (Vsx2)	Goat	Retinal progenitor cells	1:100	Santa Cruz Biotechnology, Dallas, TX
CRALBP (cellular retinaldehyde binding protein)	Rabbit	Müller glial cells and retinal pigment epithelium	1:1000	Gift of Dr. Saari, Univ. of Washington, Seattle, WA [58]
GFAP (Glial fibrillary acidic protein)	Rabbit	Glial cells (in retina, astrocytes, and reactive Müller cells)	1:2000	Chemicon, Temecula, CA
Glutamine synthetase	Mouse	Glial cells	1:1000	Transduction Laboratories, Lexington KY (now BD Biosciences, San Jose, CA)
Human nuclei	Mouse	Human cells	1:1000	Chemicon
Human nuclei (Ku-80)	Rabbit	Human cells	1:400	Abcam, Cambridge, MA
Human neurofilament (NF)	Rabbit	Human neurofilament 160 kD (does not stain rat)—marker for human neurons	1:200	Epitomics
MAP2	Mouse	Microtubule-associated protein 2 (neuronal marker)	1:200–1:500	Chemicon
NeuN (neuronal nuclei)	Mouse	Neurons	1:400	Chemicon
NRL (Neural retina-specific leucine zipper protein)	Rabbit	Transcription factor regulating rod-photoreceptor-specific genes	1:1000	Gift of Dr. Swaroop, NEI, Bethesda, MD [59]
Otx2 (orthodenticle homolog 2 homeobox protein)	Rabbit	Transcription factor in forebrain and eye development	1:1000	Chemicon
Pax 6	Rabbit	Transcription factor pax 6	1:500	Chemicon
Protein kinase C (PKC) α	Mouse	Rod bipolar cells	1:200	StressGen Bioreagents, Ann Arbor, MI
Recoverin	Rabbit	Rod and cone photoreceptors, cone bipolar cells	1:500	Gift of Dr. Dizhoor, Salus Univ, PA [60]
Red-green opsin	Rabbit	Red-green-sensitive cones	1:2000	Chemicon
Rhodopsin (clone rho1D4)	Mouse	Rod photoreceptors	1:50	Gift of Dr. Molday, Univ. of British Columbia [61]
Vimentin	Mouse	Intermediate filament vimentin	1:500	ICN, Aurora, OH (now MP Biomedicals, Santa Ana, CA)
Secondary antibodies				
Rhodamine X anti-mouse	Goat	Mouse antibodies	1:200	Molecular Probes, Eugene, OR
AF488 anti rabbit	Goat	Rabbit antibodies	1:200	Molecular Probes
Cy2-anti goat	Rabbit	Goat antibodies	1:200	Jackson ImmunoResearch, West Grove, PA

Characterization of hESC-derived neural progenitor sheets used for transplantation

Many cells of the hESC-derived neural progenitor sheets stained for the neural nuclei marker NeuN and the transcription factor Pax 6 at day 44 of differentiation (Fig. 4a), and for the neuronal marker MAP2 at day 36 of differentiation (Fig. 4b) The intermediate filament Vimentin was expressed by all cells at day 36 (Fig. 4b). At day 36, some cellular processes were stained for cellular retinaldehyde binding protein (CRALBP), a marker of RPE cells and Müller glia (Fig. 4c). Many cells were stained for Chx10 (vsx2), a transcription factor specific for retinal progenitor cells at day 44 (Fig. 4d), and Otx2, a transcription factor in forebrain and eye development at day 36 (Fig. 4e). Very few cells were stained for the photoreceptor precursor-specific transcription factors NRL at day 44 (Fig. 4f). No stain was found for more mature cell markers such as recoverin (Fig. 4e), glutamine synthetase (Fig. 4f), rhodopsin, or protein kinase C alpha (data not shown).

hESC-derived neural progenitor sheet transplants in RD nude and NIH nude rats

Recipients of sheet transplants survived well; only one rat died of unknown causes at 4.1 months after surgery

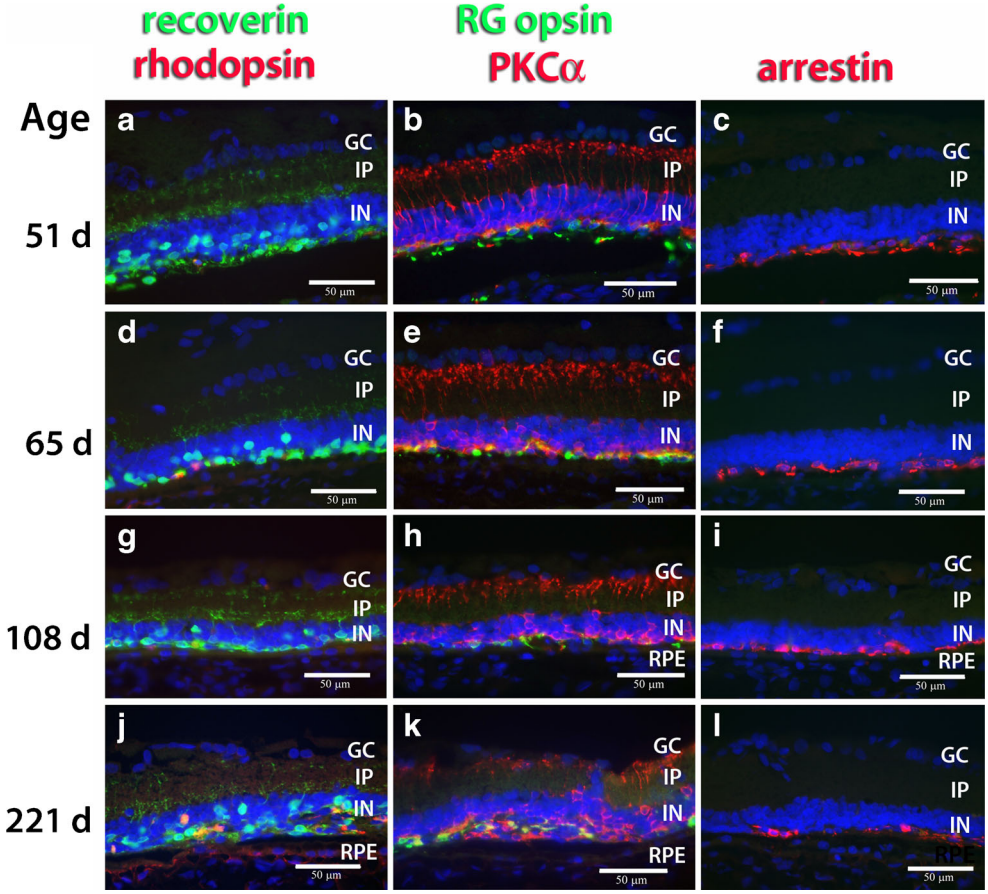

Fig. 3 Retinal degeneration in RD nude rats. Immunohistochemistry for different retinal markers in central retina at the ages of 51 days (**a**, **b**, **c**), 65 days (**d**, **e**, **f**), 108 days (**g**, **h**, **i**), and 221 days (**j**, **k**, **l**). Nuclei are labeled *blue*. Left column (**a**, **d**, **g**, **j**): recoverin (*green*; photoreceptors and cone bipolar cells) and rhodopsin (*red*; rods). Middle column (**b**, **e**, **h**, **k**): red-green opsin (*green*; red-green cones) and PKCα (red; rod bipolar cells). Right column (**c**, **f**, **i**, **l**): arrestin (S-antigen, *red*; photoreceptors). Most rods (α rhodopsin) are lost at the age of 51 days; very few scattered rods are remaining at later ages. Cones (α-recoverin, α-RG opsin, α-arrestin) are gradually lost at later ages. Severe retinal remodeling at the age of 7.4 months (221 days). *Bars* = 50 µm. *GC* ganglion cell layer, *IP* inner plexiform layer, *IN* inner nuclear layer, *RPE* retinal pigment epithelium

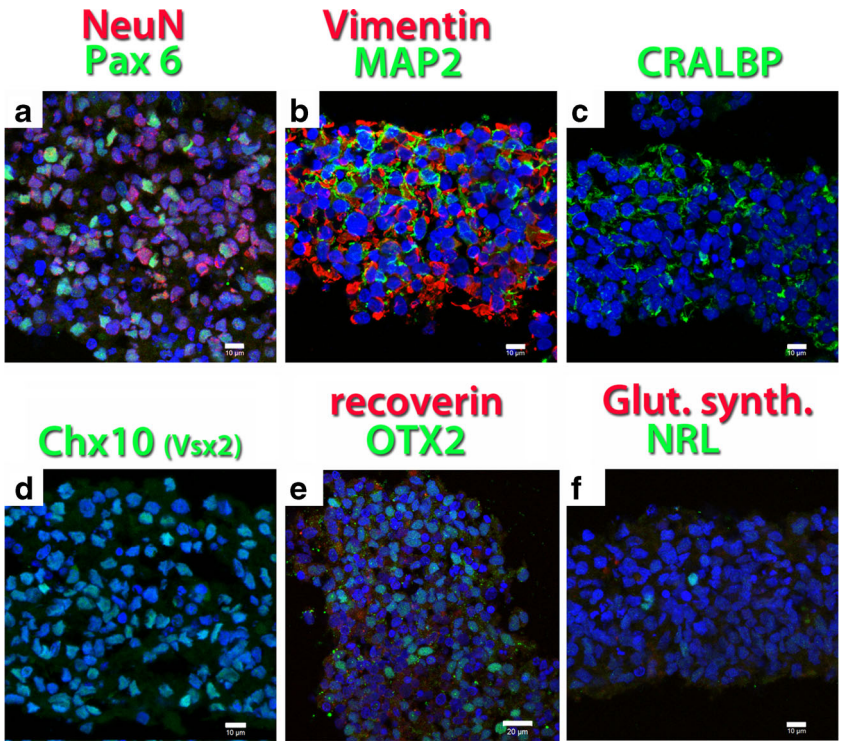

Fig. 4 hESC-derived neural progenitor sheets used for transplantation, differentiated for 36–44 days. Confocal projections. Nuclei are labeled blue. **a** Neuronal marker NeuN (*red*), transcription factor Pax 6 (*green*) (d44). **b** Intermediate filament Vimentin (*red*), marker for neuronal processes MAP2 (*green*) (d36). **c** Marker for Müller glia- and RPE, cellular retinaldehyde binding protein CRALBP (*green*) (d36). **d** More than 50 % of the cells stain for the retinal progenitor transcription factor Chx10 (Vsx2) (*green*) (d44). **e** No specific stain for recoverin (*red*); clear stain for transcription factor Otx2 (*green*) (d36). **f** No specific stain for glial marker glutamine synthetase (*red*), few cells labeled for photoreceptor precursor transcription factor NRL (*green*) (d44). *Bars* = 10 µm (**a**–**d**, **f**); *bar* = 20 µm (**e**)

Table 2 Overview of transplant experiments

Rat type	Age at surgery	Survival time	Results	
RD nude rats: 8 F, 4 M	39–43 days	8–176 days (0.3–5.9 months)	One rat found dead at 122 days (4.1 months) post-surgery; large transplants in 8 rats; small grafts in 4	
NIH nude rats: 8 F	43–51 days	0–184 days (0–6.1 months)	One rat terminated after surgery (hit optic nerve); one rat died after surgery (anesthesia); large transplants in five rats; one graft in vitreous	
		All	RD nude rats	NIH nude rats
Transplant size at implantation		1.08±0.07 mm^2 (SD) n=20	1.06±0.03 mm^2 (SD) n=12	1.12±0.11 mm^2 (SD) n=8
Transplant size at dissection	8–22 days (0.3–0.7 month)	1.65±0.88 mm^2 (SD) n=4	2.98±2.6 mm^2 (SD) n=5	3.09±0.24 mm^2 (SD) n=3
	26–42 days (0.9–1.4 months)	4.39±1.81 mm^2 (SD) n=4		
	63–88 days (2.2–2.9 months)	3.72±1.42 mm^2 (SD) n=4	5.51±1.61 mm^2 (SD) n=5	3.78±2.11 mm^2 (SD) n=3
	104–184 days (3.5–6.1 months)	6.41±1.63 mm^2 (SD) n=4		
Total transplant size at dissection	8–184 days (0.3–6.1 months)	4.04±2.2 mm^2 (SD) n=16	4.24±2.42 mm^2 (SD) n=10	3.71±1.9 mm^2 (SD) n=6

(see Table 2). Transplants formed whitish tissues and grew in size to cover up to a sixfold portion of the original area (Table 2, Fig. 5). Most of the growth appeared to occur at 26–28 days (0.9 months) after transplantation (Table 2).

Up to 8 days after transplantation, a clear glial boundary between transplant and host could still be observed (Fig. 6a). Although the hESC-derived neural progenitor sheets had been placed into the subretinal space, migration into the host retina was observed at 26–28 days after transplantation, both in transplants to RD nude rats (Figs. 6b, d and 7a–d) and to NIH nude rats (Fig. 8a–c). Host glial cells extended processes into the transplant and migrated into the transplant (Fig. 6b, e). Few transplant cells were immunoreactive for CRALBP at 28 days after transplant (Fig. 6c), but at later stages there was more CRALBP expression (Fig. 6e). Host and transplant cells showed GFAP immunoreactivity at 26 days after surgery (Fig. 6d) and at later time points (data not shown).

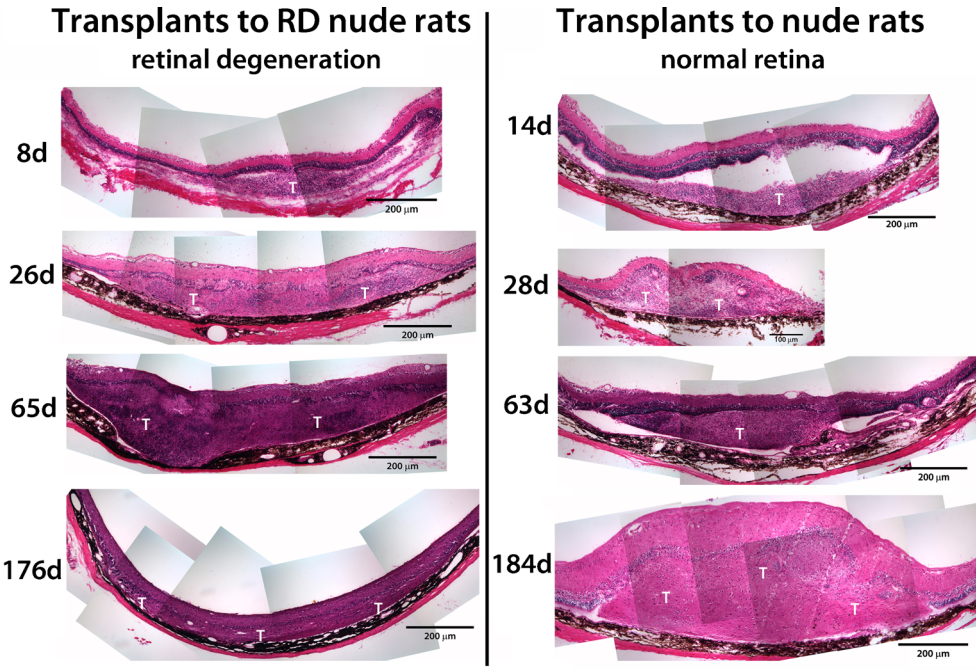

Fig. 5 Overview of hESC-derived neuronal progenitor transplants (examples of hematoxylin-eosin-stained cross sections). All images are at the same magnification, with the ganglion layer on top and the RPE on bottom. *Left column* transplants to RD nude rats (8–174 days after surgery). *Right column* transplants to NIH nude rats (14–184 days after surgery). At early stages (8 days, 14 days), transplants (T) appear separated from the host retina, but appear integrated at all later stages. The section on the *bottom right* (transplant to NIH nude rat 184 days after surgery) is tangentially cut and appears thicker

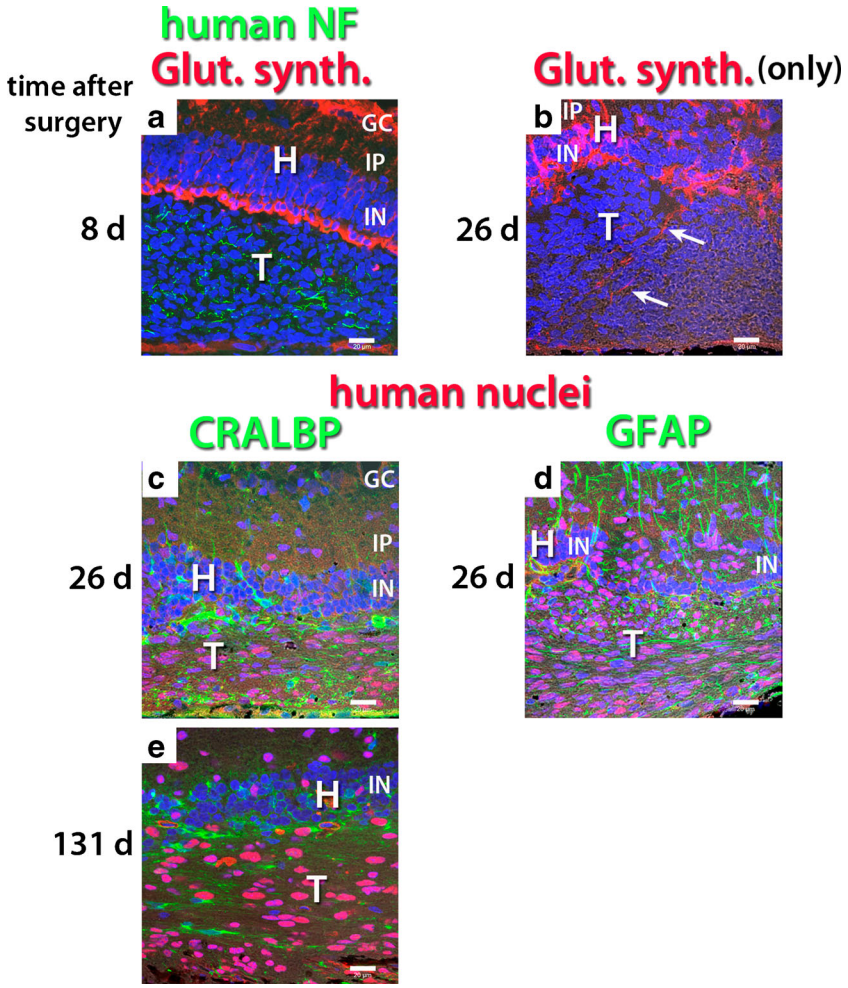

Fig. 6 Glial markers in transplants of hESC-derived neuronal progenitors in transplants to RD nude rats. All confocal images are oriented with the ganglion cell layer up and the RPE layer toward the bottom. Nuclei are labeled *blue*. **a** Human NF (*green*), glutamine synthetase (*red*), 8 days after surgery. At this stage, there is still a clear border between transplant (T) and host (H). **b** At 26 days after surgery, transplant cells have migrated into the host retina. Note the disruption of the regular arrangement of host Müller cells. Glutamine synthetase immunoreactive glial processes apparently extend from host retina into transplant (*arrows*). The donor cells are not immunoreactive for glutamine synthetase. **c**, **d**, **e** CRALBP (*green*) in combination with human nuclei (*red*). **c** At 26 days after surgery, few CRALBP immunoreactive cells are seen in the transplant. **d** GFAP (*green*) in combination with human nuclei (*red*), 26 days after surgery. Extensive expression of GFAP in transplant and host. In the host inner plexiform and inner nuclear layers, the regular radial processes are host Müller cell processes, the irregular processes are likely derived from the transplant. Donor cells have migrated into the host retina. **e** At 131 days after surgery, host-derived CRALBP+cells (not staining for human nuclei) are found inside transplant, but there are also *CRALBP-expressing* donor cells. *Bars* = 20 μm. *GC* ganglion cell layer, *IP* inner plexiform layer, *IN* inner nuclear layer, *H* host, *T* transplant

Neuronal processes of human donor cells, clearly identified by antibodies for ß-III-tubulin (Figs. 7a and 8a) and by an antibody specific for human neurofilament, i.e., human neuronal processes (Figs. 7e, i and 8d, g), were very dense in the transplant area and extended into the host inner plexiform layer. These donor processes were also immunoreactive to MAP2, a marker for neuronal processes (Fig. 7c, g, k). Donor cells did not express the retina-specific marker recoverin (Figs. 7b, f, g and 8b, e, h), which labeled host photoreceptors (remaining cones in RD nude rats and rods and cones in NIH nude rats) and cone bipolar cells. The hESC-derived neural progenitor cells migrated extensively from the transplant sheets throughout the host retina, which eventually resulted in the loss of the host retinal structure in the RD nude rats (Fig. 7f–k). NIH nude rats partially lost their outer nuclear layer over the transplant (Fig. 8b, e, h). Migration was much more extensive in RD nude than in NIH nude rats (data not shown). Transplant cells did not express PKCα, a marker for rod bipolar cells in the retina, at 26–28 days after surgery (Figs. 7d and 8c), but showed dense PKCα-immunoreactive processes at later time points (Figs. 7h, l and 8f, i). The morphology of transplant PKCα-immunoreactive cells was completely different from host rod bipolar cells.

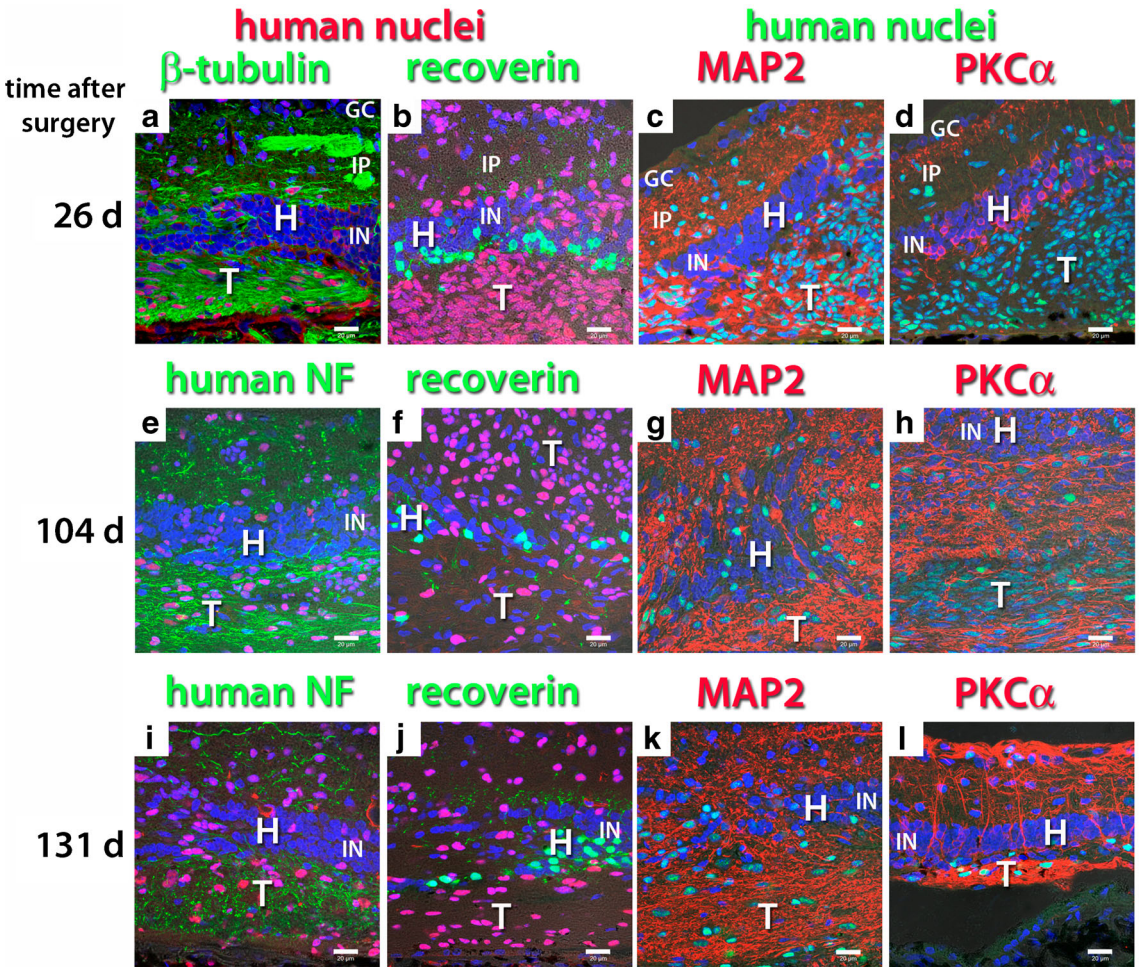

Fig. 7 Neuronal markers in transplants of hESC-derived neuronal progenitors to RD nude rats. Confocal projections. Nuclei are labeled *blue*. The figure is arranged in four columns according to the antibody combination and in three rows according to time after surgery. **a**, **b**, **c** 26 days after surgery. Migration of donor cells into inner plexiform layer of the host. **d**, **e**, **f** 104 days after surgery. The structure of host retina is dissolving due to migrating graft cells and processes. **g**, **h**, **i** 131 days after surgery. **a** Human nuclei (*red*), beta-tubulin (*green*). The transplant shows dense immunoreactivity for ß-tubulin, with processes and nerve fiber bundles extending into the host inner plexiform layer. **e**, **i** Human nuclei (*red*), human neurofilament (NF, *green*). Host inner plexiform layer filled with donor-derived neuronal processes. **b**, **f**, **j** Human nuclei (*red*), recoverin (*green*). Strong staining of remaining host cones and cone bipolar cells. Donor cells do not express recoverin. **c**, **g**, **k** Human nuclei (*green*), MAP2 (*red*). Donor cells form a dense network of neuronal processes. **d**, **h**, **l** Human nuclei (*green*), PKCα (*red*). Although donor cells do not express PKCα at 26 days after surgery (**d**), they show strong expression at later time points (**h**, **l**). However, their morphology is completely different from the retinal rod bipolar cells. **l** Edge of transplant penetrating host retina with numerous processes. *Bars* = 20 μm. *GC* ganglion cell layer, *IP* inner plexiform layer, *IN* inner nuclear layer, *H* host, *T* transplant

Discussion

A new immunodeficient retinal degenerate rat strain has been created that will be useful in studying the effect of human cell transplantation, especially on restoration of visual responses.

Retinal diseases affect millions of people. Once photoreceptors have degenerated, they cannot be regenerated. Transplantation of fetal retinal sheets together with and without its RPE has resulted in visual improvements in animal models (review [17–19]) and in human patients [20]. Several laboratories are working on transplantation of human stem cell-derived retinal progenitors or RPE cells with the goal of restoring vision using mostly immunosuppressed animal models [22–25, 27, 35, 41–43]. However, immunosuppression is very labor-intensive and can have negative effects on the health of the recipient, especially with long-term use; e.g., the most commonly used immunosuppressant cyclosporin A can have nephrotoxic effects [44, 45]. Thus, it would be advantageous to have an immunodeficient rat model of retinal degeneration. This is the first time that such a model has been created.

Due to the limited number of animals available, we have not been able to obtain data from earlier stages of retinal degeneration in this rat model. PCR data cannot distinguish between homozygous and hemizygous expression of the S334ter-transgene. However, the available histology clearly

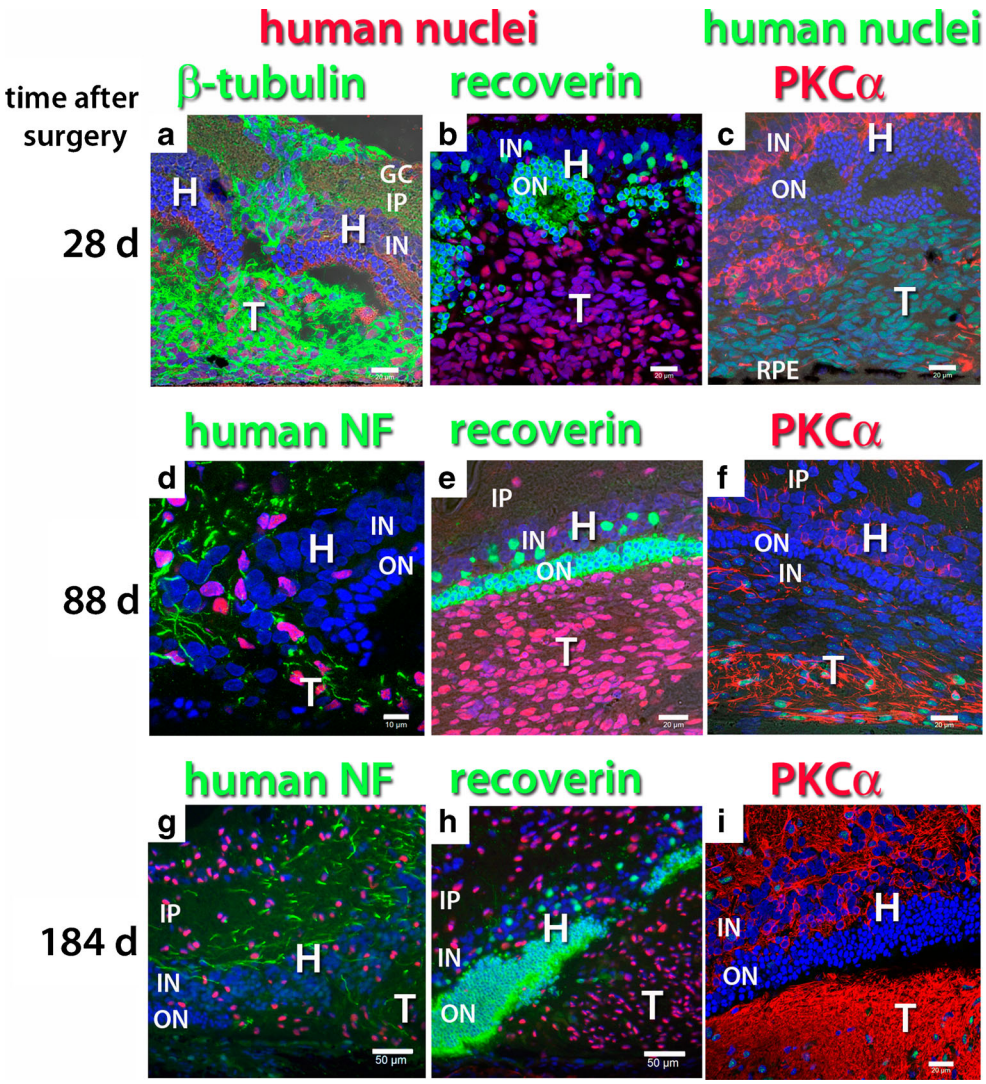

Fig. 8 Neuronal markers in transplants of hESC-derived neuronal progenitors to NIH nude rats. **a**–**f**, **i** Confocal projections; **g**, **h** standard fluorescence micrographs. Nuclei are labeled *blue*. The figure is arranged in three columns according to the antibody combination and in three rows according to time after surgery. **a**, **b**, **c** 28 days after surgery. Migration of donor cells into host. **d**, **e**, **f** Eighty-eight days after surgery. Further migration of donor cells, penetration of host retina with graft processes, structure of host retina disintegrating. **g**, **h**, **i** 184 days after surgery. **a** Human nuclei (*red*), beta-tubulin (*green*). Donor processes extending from subretinal transplant through host retina towards vitreous. **d**, **g** Human nuclei (*red*), human neurofilament (NF, *green*). **b**, **e**, **h** Human nuclei (*red*), recoverin (*green*). The remaining host outer nuclear layer stains strongly for recoverin. Donor cells do not express recoverin. In **b**, the host outer nuclear layer is partially dissolved, in **e** and **h**, it has become thinner. **c**, **f**, **i** Human nuclei (*green*), PKCα (*red*). **c** Donor cells do not express PKCα at 28 days after surgery, when host bipolar cells extend processes into the transplant in some areas. **f**, **i** PKC expression of the transplant increases between 88 and 184 days. *Bars* = 10 µm (**d**), = 20 µm (**a**, **b**, **c**, **d**, **e**, **f**, **i**); *Bars* = 50 µm. (**g**, **h**). *GC* ganglion cell layer, *IP* inner plexiform layer, *IN* inner nuclear layer, *ON* outer nuclear layer, *RPE* retinal pigment epithelium, *H* host, *T* transplant

indicates that the retinal degeneration in RD nude rats (SD-Foxn1Tg(S334ter)3Lav) follows the same pattern as in the original S334ter line 3 rat strain SD-Tg(S334ter)3Lav [31].

The athymic nude rat (*Foxn1*$^{rnu/rnu}$) is a popular model to test xenografts of human tissue [35–37, 46, 47]. However, it has a normal retina and therefore the effect of retinal transplants on visual restoration cannot be tested. Our laboratory has tried previously in vain to create a nude rat light damage model using continuous blue light (unpublished data). Photoreceptor death due to light damage apparently requires T-cells.

Other researchers have created immunodeficient disease models, mostly with mouse strains, mainly in tumor models [48] or in models of CNS disease and injury [49] (review [50]). However, so far there is no report of an immunodeficient retinal degeneration model.

The hESC-derived neural progenitor cells used in this study were clearly too immature as indicated by their widespread migration and proliferation and did not develop into retinal neurons. However, our data demonstrate that these immature cells could further differentiate and migrate

extensively throughout the retina and into the choroid. The cells did not express PKCα at early time points, but showed strong PKC expression later. It has been shown that human neural progenitors migrate much further distances than rat or mouse neural progenitor cells in the nude rat brain [49]. This was similar to what was seen in our study.

Future experiments will involve transplanting sheets of hESC-derived retinal progenitor cells, using improved protocols that can achieve "laminated" structures with photoreceptor precursors [25, 28, 51].

Since this rat strain loses its rods early on, "direct effects" due to reconnection and "indirect effects" due to trophic factors can be distinguished by studying rod-specific visual responses, and by including controls with injecting trophic factors, and/or transplanting non-retinal neural progenitors. Several papers have demonstrated this point with transplants of rat fetal tissue (e.g., [52, 53]). In any case, the point is that this rat strain allows studying the effects of human cell transplants on visual responses whether they act via trophic or direct replacement effects, without the interference of immunosuppressants.

The subretinal space, similar to the brain, was previously considered to be "immune privileged" [54], i.e., allografts of fetal retina or retinal progenitor cells survive in the subretinal space without immunosuppression [55]. Xenografts to the brain of newborn animals without a developed immune system are immunologically tolerated and survive unless the host is challenged [56]. Hambright et al. showed that xenografts of dissociated hESC-derived retinal progenitor cells can survive in the subretinal space without immunosuppression provided there is no break in the blood–retinal barrier [27]. However, their surgical approach through the cornea is not compatible with human vitreoretinal surgery.

Conclusions

This newly created immunodeficient rat model with retinal degeneration is useful for testing transplantation of human cells for improving or restoring vision. It can be used for various experimental approaches, transplantation of photoreceptor precursors, neural progenitor cells, or retinal progenitor sheets. Importantly, the RD nude rat provides a robust and improved animal model for the study of retinal degeneration and transplantation with better health than immunosuppressed rats. At the RRRC, it was not necessary to take extra measures like maintaining sterility while maintaining the rats under pathogen-free conditions in microisolator cages.

Acknowledgments This work was supported by the Lincy Foundation (MJS, HSK); NIH P40OD011062 (ECB). Access to the Optical Biology Core facility of the Developmental Biology Center, a Shared Resource, was supported in part by a Cancer Center Support Grant (CA-62203) and a Center for Complex Biological Systems Support Grant (GM-076516) at the University of California, Irvine. MKJ was supported by CIRM TB1-1182. We thank Matthew M. LaVail, UCSF, for the founder breeding pairs of transgenic S334ter line 3 rats. The initial breeding of the strain was done at Taconic Inc., Albany, NY, USA. Personnel of Taconic involved in the project included Kaitlyn Waterbury, Jacob Luft, and Kimberly Meagher. We thank Gabriel Nistor (now California Stem Cells Inc., Irvine, CA, USA) for designing the hESC differentiation protocol and preparing the cells for transplantation.

Conflict of interest MJS and RBA have proprietary interests in the implantation instrument and procedure (Ocular Transplantation LLC; patents #5,941,250; 6,159,218; 6,156,042); RBA is also an employee of Ocular Transplantation LLC. HSK was on the scientific advisory board of California Stem Cell, Inc. at the time of the experiments; and is now President and Chief Executive Officer of California Stem Cell, Inc. since December 2013.

References

1. Nussenblatt RB, Liu B, Li Z (2009) Age-related macular degeneration: an immunologically driven disease. Curr Opin Investig Drugs 10:434–442
2. Sahel J, Bonnel S, Mrejen S, Paques M (2010) Retinitis pigmentosa and other dystrophies. Dev Ophthalmol 47:160–167. doi:10.1159/000320079
3. Huang Y, Enzmann V, Ildstad ST (2011) Stem cell-based therapeutic applications in retinal degenerative diseases. Stem Cell Rev 7:434–445. doi:10.1007/s12015-010-9192-8
4. Kokotas H, Grigoriadou M, Petersen MB (2011) Age-related macular degeneration: genetic and clinical findings. Clin Chem Lab Med 49:601–616. doi:10.1515/CCLM.2011.091
5. Trifunovic D, Sahaboglu A, Kaur J, Mencl S, Zrenner E, Ueffing M, Arango-Gonzalez B, Paquet-Durand F (2012) Neuroprotective strategies for the treatment of inherited photoreceptor degeneration. Curr Mol Med 12:598–612
6. Sin HP, Liu DT, Lam DS (2012) Lifestyle modification, nutritional and vitamins supplements for age-related macular degeneration. Acta Ophthalmol. doi:10.1111/j.1755-3768.2011.02357.x
7. Wen R, Tao W, Li Y, Sieving PA (2012) CNTF and retina. Prog Retin Eye Res 31:136–151. doi:10.1016/j.preteyeres.2011.11.005
8. Thanos C, Emerich D (2005) Delivery of neurotrophic factors and therapeutic proteins for retinal diseases. Expert Opin Biol Ther 5:1443–1452. doi:10.1517/14712598.5.11.1443
9. LaVail MM (2005) Survival factors for treatment of retinal degenerative disorders: preclinical gains and issues for translation into clinical studies. Retina 25:S25–S26
10. Lund R (2008) Cell-based therapies to limit photoreceptor degeneration. Arch Soc Esp Oftalmol 83:457–464
11. Schwartz SD, Hubschman JP, Heilwell G, Franco-Cardenas V, Pan CK, Ostrick RM, Mickunas E, Gay R, Klimanskaya I, Lanza R (2012) Embryonic stem cell trials for macular degeneration: a preliminary report. Lancet 379:713–720. doi:10.1016/S0140-6736(12)60028-2
12. Klassen HJ, Ng TF, Kurimoto Y, Kirov I, Shatos M, Coffey P, Young MJ (2004) Multipotent retinal progenitors express developmental markers, differentiate into retinal neurons, and preserve light-mediated behavior. Invest Ophthalmol Vis Sci 45:4167–4173. doi:10.1167/iovs.04-0511
13. Singh MS, Charbel Issa P, Butler R, Martin C, Lipinski DM, Sekaran S, Barnard AR, MacLaren RE (2013) Reversal of end-stage retinal degeneration and restoration of visual function by photoreceptor transplantation. Proc Natl Acad Sci U S A 110:1101–1106. doi:10.1073/pnas.1119416110

14. Lamba DA, Gust J, Reh TA (2009) Transplantation of human embryonic stem cell-derived photoreceptors restores some visual function in Crx-deficient mice. Cell Stem Cell 4:73–79. doi:10.1016/j.stem.2008.10.015
15. MacLaren RE, Pearson RA, MacNeil A, Douglas RH, Salt TE, Akimoto M, Swaroop A, Sowden JC, Ali RR (2006) Retinal repair by transplantation of photoreceptor precursors. Nature 444:203–207
16. Mansergh FC, Vawda R, Millington-Ward S, Kenna PF, Haas J, Gallagher C, Wilson JH, Humphries P, Ader M, Farrar GJ (2010) Loss of photoreceptor potential from retinal progenitor cell cultures, despite improvements in survival. Exp Eye Res 91:500–512. doi:10.1016/j.exer.2010.07.003
17. Aramant RB, Seiler MJ (2004) Progress in retinal sheet transplantation. Prog Retin Eye Res 23:475–494
18. Seiler MJ, Aramant RB, Keirstead HS (2008) Retinal transplants: hope to preserve and restore vision? Opt Photonics News 19:37–47
19. Seiler MJ, Aramant RB (2012) Cell replacement and visual restoration by retinal sheet transplants. Prog Retin Eye Res 31:661–687. doi:10.1016/j.preteyeres.2012.06.003
20. Radtke ND, Aramant RB, Petry HM, Green PT, Pidwell DJ, Seiler MJ (2008) Vision improvement in retinal degeneration patients by implantation of retina together with retinal pigment epithelium. Am J Ophthalmol 146:172–182. doi:10.1016/j.ajo.2008.04.009
21. Meyer JS, Shearer RL, Capowski EE, Wright LS, Wallace KA, McMillan EL, Zhang SC, Gamm DM (2009) Modeling early retinal development with human embryonic and induced pluripotent stem cells. Proc Natl Acad Sci U S A 106:16698–16703. doi:10.1073/pnas.0905245106
22. Yue F, Johkura K, Shirasawa S, Yokoyama T, Inoue Y, Tomotsune D, Sasaki K (2010) Differentiation of primate ES cells into retinal cells induced by ES cell-derived pigmented cells. Biochem Biophys Res Commun 394:877–883. doi:10.1016/j.bbrc.2010.03.008
23. Lamba DA, McUsic A, Hirata RK, Wang PR, Russell D, Reh TA (2010) Generation, purification and transplantation of photoreceptors derived from human induced pluripotent stem cells. PLoS One 5:e8763. doi:10.1371/journal.pone.0008763
24. Tucker BA, Park IH, Qi SD, Klassen HJ, Jiang C, Yao J, Redenti S, Daley GQ, Young MJ (2011) Transplantation of adult mouse iPS cell-derived photoreceptor precursors restores retinal structure and function in degenerative mice. PLoS One 6:e18992. doi:10.1371/journal.pone.0018992
25. Meyer JS, Howden SE, Wallace KA, Verhoeven AD, Wright LS, Capowski EE, Pinilla I, Martin JM, Tian S, Stewart R, Pattnaik B, Thomson JA, Gamm DM (2011) Optic vesicle-like structures derived from human pluripotent stem cells facilitate a customized approach to retinal disease treatment. Stem Cells 29:1206–1218. doi:10.1002/stem.674
26. Parameswaran S, Balasubramanian S, Babai N, Qiu F, Eudy JD, Thoreson WB, Ahmad I (2010) Induced pluripotent stem cells generate both retinal ganglion cells and photoreceptors: therapeutic implications in degenerative changes in glaucoma and age-related macular degeneration. Stem Cells 28:695–703. doi:10.1002/stem.320
27. Hambright D, Park KY, Brooks M, McKay R, Swaroop A, Nasonkin IO (2012) Long-term survival and differentiation of retinal neurons derived from human embryonic stem cell lines in un-immunosuppressed mouse retina. Mol Vis 18:920–936
28. Nakano T, Ando S, Takata N, Kawada M, Muguruma K, Sekiguchi K, Saito K, Yonemura S, Eiraku M, Sasai Y (2012) Self-formation of optic cups and storable stratified neural retina from human ESCs. Cell Stem Cell 10:771–785. doi:10.1016/j.stem.2012.05.009
29. Steinberg RH, Flannery JG, Naash M, Oh P, Matthes MT, Yasumura D, Lau-Villacorta C, Chen J, LaVail MM (1996) Transgenic rat models of inherited retinal degeneration caused by mutant opsin genes [ARVO abstract]. Invest Ophthalmol Vis Sci 37:S698
30. Pennesi ME, Nishikawa S, Matthes MT, Yasumura D, LaVail MM (2008) The relationship of photoreceptor degeneration to retinal vascular development and loss in mutant rhodopsin transgenic and RCS rats. Exp Eye Res 87:561–570. doi:10.1016/j.exer.2008.09.004
31. Martinez-Navarrete G, Seiler MJ, Aramant RB, Fernandez-Sanchez L, Pinilla I, Cuenca N (2011) Retinal degeneration in two lines of transgenic S334ter rats. Exp Eye Res 92:227–237. doi:10.1016/j.exer.2010.12.001
32. Segre JA, Nemhauser JL, Taylor BA, Nadeau JH, Lander ES (1995) Positional cloning of the nude locus: genetic, physical, and transcription maps of the region and mutations in the mouse and rat. Genomics 28:549–559. doi:10.1006/geno.1995.1187
33. Hirasawa T, Yamashita H, Makino S (1998) Genetic typing of the mouse and rat nude mutations by PCR and restriction enzyme analysis. Exp Anim 47:63–67
34. Aramant RB, Seiler MJ (1994) Human embryonic retinal cell transplants in athymic immunodeficient rat hosts. Cell Transplant 3:461–474
35. Guest JD, Rao A, Olson L, Bunge MB, Bunge RP (1997) The ability of human Schwann cell grafts to promote regeneration in the transected nude rat spinal cord. Exp Neurol 148:502–522. doi:10.1006/exnr.1997.6693
36. Aramant RB, Seiler MJ (2002) Transplanted sheets of human retina and retinal pigment epithelium develop normally in nude rats. Exp Eye Res 75:115–125
37. Nasonkin I, Mahairaki V, Xu L, Hatfield G, Cummings BJ, Eberhart C, Ryugo DK, Maric D, Bar E, Koliatsos VE (2009) Long-term, stable differentiation of human embryonic stem cell-derived neural precursors grafted into the adult mammalian neostriatum. Stem Cells 27:2414–2426. doi:10.1002/stem.177
38. Liang SC, Lin SZ, Yu JF, Wu SF, Wang SD, Liu JC (1997) F344-rnu/rnu athymic rats: breeding performance and acceptance of subcutaneous and intracranial xenografts at different ages. Lab Anim Sci 47:549–553
39. Nistor G, Seiler MJ, Yan F, Ferguson D, Keirstead HS (2010) Three-dimensional early retinal progenitor 3D tissue constructs derived from human embryonic stem cells. J Neurosci Methods 190:63–70. doi:10.1016/j.jneumeth.2010.04.025
40. Aramant RB, Seiler MJ (2002) Retinal transplantation—advantages of intact fetal sheets. Prog Retin Eye Res 21:57–73
41. Lamba DA, Karl MO, Ware CB, Reh TA (2006) Efficient generation of retinal progenitor cells from human embryonic stem cells. Proc Natl Acad Sci U S A 103:12769–12774
42. Vugler AA (2010) Progress toward the maintenance and repair of degenerating retinal circuitry. Retina 30:983–1001. doi:10.1097/IAE.0b013e3181e2a680
43. Clarke L, Ballios BG, van der Kooy D (2012) Generation and clonal isolation of retinal stem cells from human embryonic stem cells. Eur J Neurosci 36:1951–1959. doi:10.1111/j.1460-9568.2012.08123.x
44. Thliveris JA, Yatscoff RW, Lukowski MP, Copeland KR (1991) Cyclosporine nephrotoxicity–experimental models. Clin Biochem 24:93–95
45. Cibulskyte D, Kaalund H, Pedersen M, Horlyck A, Marcussen N, Hansen HE, Madsen M, Mortensen J (2005) Chronic cyclosporine nephrotoxicity: a pig model. Transplant Proc 37:3298–3301. doi:10.1016/j.transproceed.2005.09.004
46. Granholm AC, Eriksdotter-Nilsson M, Stromberg I, Stieg P, Seiger A, Bygdeman M, Geffard M, Oertel W, Dahl D, Olson L et al (1989) Morphological and electrophysiological studies of human hippocampal transplants in the anterior eye chamber of athymic nude rats. Exp Neurol 104:162–171
47. Hall M, Wang Y, Granholm AC, Stevens JO, Young D, Hoffer BJ (1992) Comparison of fetal rabbit brain xenografts to three different strains of athymic nude rats: electrophysiological and immunohistochemical studies of intraocular grafts. Cell Transplant 1:71–82
48. Kim M, Park IY, Lim J, Kim Y, Han KT, Chung WH, Han K (2006) Antitumor and normal cell protective effect of PKC412 in the

athymic mouse model of ovarian cancer. Ann Clin Lab Sci 36:455–460
49. Hurelbrink CB, Barker RA (2005) Migration of cells from primary transplants of allo- and xenografted foetal striatal tissue in the adult rat brain. Eur J Neurosci 21:1503–1510. doi:10.1111/j.1460-9568.2005.03963.x
50. Anderson AJ, Haus DL, Hooshmand MJ, Perez H, Sontag CJ, Cummings BJ (2011) Achieving stable human stem cell engraftment and survival in the CNS: is the future of regenerative medicine immunodeficient? Regen Med 6:367–406. doi:10.2217/rme.11.22
51. Phillips MJ, Wallace KA, Dickerson SJ, Miller MJ, Verhoeven A, Martin JM, Wright L, Shen W, Capowski EE, Percin EF, Perez ET, Zhong X, Canto-Soler MV, Gamm DM (2012) Blood-derived human iPS cells generate optic vesicle-like structures with the capacity to form retinal laminae and develop synapses. Invest Ophthalmol Vis Sci 53:2007–2019. doi:10.1167/iovs.11-9313
52. Seiler MJ, Aramant RB, Thomas BB, Peng Q, Sadda SR, Keirstead HS (2010) Visual restoration and transplant connectivity in degenerate rats implanted with retinal progenitor sheets. Eur J Neurosci 31:508–520. doi:10.1111/j.1460-9568.2010.07085.x
53. Yang PB, Seiler MJ, Aramant RB, Yan F, Mahoney MJ, Kitzes LM, Keirstead HS (2010) Trophic factors GDNF and BDNF improve function of retinal sheet transplants. Exp Eye Res 91:727–738. doi:10.1016/j.exer.2010.08.022
54. Niederkorn JY (2006) See no evil, hear no evil, do no evil: the lessons of immune privilege. Nat Immunol 7:354–359. doi:10.1038/ni1328
55. Lund RD, Ono SJ, Keegan DJ, Lawrence JM (2003) Retinal transplantation: progress and problems in clinical application. J Leukoc Biol 74:151–160
56. Banerjee R, Lund RD, Radel JD (1993) Anatomical and functional consequences of induced rejection of intracranial retinal transplants. Neuroscience 56:939–953
57. Donoso LA, Merryman CF, Edelberg KE, Naids R, Kalsow C (1985) S-Antigen in the developing retina and pineal gland: a monoclonal antibody study. Invest Ophthalmol Vis Sci 26:561–567
58. Saari JC, Bunt-Milam AH, Bredberg DL, Garwin GG (1984) Properties and immunocytochemical localization of three retinoid-binding proteins from bovine retina. Vis Res 24:1595–1603
59. Mears AJ, Kondo M, Swain PK, Takada Y, Bush RA, Saunders TL, Sieving PA, Swaroop A (2001) Nrl is required for rod photoreceptor development. Nat Genet 29:447–452. doi:10.1038/ng774
60. Dizhoor AM, Ray S, Kumar S, Niemi G, Spencer M, Brolley D, Walsh KA, Philipov PP, Hurley JB, Stryer L (1991) Recoverin: a calcium sensitive activator of retinal rod guanylate cyclase. Science 251:915–918
61. Molday RS, MacKenzie D (1983) Monoclonal antibodies to rhodopsin: characterization, cross-reactivity, and application as structural probes. Biochemistry 22:653–660